Taking theory to the field: streamflow generation mechanisms in an intermittent, Mediterranean catchment

Karina Y. Gutierrez-Jurado[1], Daniel Partington[1], Margaret Shanafield[1]

[1]College of Science and Engineering, Flinders University, Adelaide, 5001, Australia

5   *Correspondence to*: Margaret Shanafield (Margaret.shanafield@flinders.edu.au)

Abstract. Understanding streamflow dynamics at the catchment scale remains an arduous task; this is especially true for non-perennial networks. While modelling tools offer important advantages to study streamflow dynamics, the highly nonlinear, unsaturated dynamics associated with the transitions between wetting and drying in non-perennial systems make modelling cumbersome. This has stifled previous modelling attempts and alludes to why there is still a knowledge gap. In this study, we

10   first construct a conceptual model of the physical processes of streamflow generation in an intermittent river system in South Australia, based on the hypothesis that the vertical and longitudinal soil heterogeneity and topography in a basin control short-term (fast flows), seasonal (slow flow), and a mixture of these two. We then construct and parameterise a fully integrated surface-subsurface hydrologic model to examine patterns and mechanisms of streamflow generation within the catchment. A set of scenarios are explored to understand the influences of topography and soil heterogeneity across the catchment. The

15   results showed distinct flow generation mechanisms develop in the three conceptualized areas with marked soil and topographic characteristics, and suggested that capturing the overall distribution of soil types across the catchment was more important than capturing the wide variability of soil hydraulic properties. This study augments our understanding of catchment scale streamflow generation processes, while also providing insight on the challenges of implementing physically-based, integrated surface-subsurface hydrological models in non-perennial stream catchments.

20   **1   Introduction**

In a world of increasing water scarcity, understanding the hydrology of rivers in arid and semi-arid regions has become increasingly important. In these regions, most streams and rivers are non-perennial, meaning surface flow ceases for some or most of the year. It is widely recognised that our hydrologic understanding of these non-perennial streams is still insufficient (Costigan et al., 2017). In particular, our understanding of the processes that lead to streamflow generation in non-perennial

25   rivers is incomplete (Gutierrez-Jurado et al., 2019; Shanafield et al., in press). This is partly due to lack of appropriate data; indeed, it has been shown that streamflow gauges, ~~which provide the most fundamental data to understanding the hydrology of~~ rivers, are preferentially located on perennial rivers (Fekete and Vörösmarty, 2002; Poff et al., 2006). In addition, the

particular challenges associated with characterising unsaturated flow, the natural wetting and drying cycles, and other highly non-linear processes complicate the efforts to model non-perennial systems (Beven, 2002; Ye et al., 1997).

30 Among semi-arid regions, Mediterranean climate regions are relatively well-represented in the literature, as unlike inland regions, they have long been population centers and therefore have experienced severe anthropogenic alteration and ever increasing water demands (Merheb et al., 2016). This type of subtropical, dry summer, wet winter climate exists not only in southern Europe, but also represents much of California, South and Western coastal Australia, South Africa, and central coastal Chile (Geiger, 1961). Intermittent (i.e. those that flow seasonally) and ephemeral (i.e. those that flow only after rain events)

35 are already prevalent in these regions; however, Mediterranean climate regions are sensitive to climate change (Cudennec et al., 2007) and expected to experience significant drying due to shifting climate patterns, which will greatly impact streamflow regimes (Milly et al., 2005). Therefore, understanding of streamflow generation mechanisms in these regions is particularly needed.

Numerical models offer a method to explore the complex drivers that lead to streamflow production in a catchment. Several

40 modelling studies of non-perennial river catchments have provided insight on the role of soil cover, topography, and soil heterogeneity on runoff generation (Pierni et al., 2014; Ebel et al., 2016; Maxwell & Kollet, 2008) and on the evolution of saturated area patterns (Weill et al., 2013), as well as the importance of unsaturated storage dynamics as major controls on the processes of runoff generation (Vanderkwaak & Loague 2001; Gutierrez-Jurado et al. 2019; Mirus & Loague 2013). Nevertheless, the required level of information to adequately parameterize boundary value problems have restricted the use of

45 fully integrated surface-subsurface hydrologic models (ISSHM) in non-perennial river catchments to mostly small-scale hillslope or headwater catchments (0.001-0.9 km^2). Moreover, most of these studies captured relatively short time periods ranging from 2h to 330 days. Under these approaches, the aim is to investigate the integrated system response to a set of distinctive scenarios and/or conditions (Carr et al., 2014; Di Giammarco et al., 1996; Heppner et al., 2007; Kollet et al., 2017; Mirus et al., 2009; Panday and Huyakorn, 2004) rather than to understand longer-term hydrological processes that control the

50 dry-wet transition.

Given these limitations, the overarching, spatiotemporal processes that control key catchment-level dynamics in non-perennial rivers remains a knowledge gap. For instance, in small-scale systems, the hydrological processes occurring at a given time and place (i.e. 'active' processes [Ambroise, 2004]) might be the same as those contributing to flow generation at that same time. However, in large-scale systems the hydrologic response is influenced by different surface water-groundwater travel times,

55 initial losses (e.g. evapotranspiration or infiltration) and the connectivity of the areas where hydrological processes are occurring. Consequently, the active processes occurring at a time and place do not necessarily contribute to the integrated catchment response at another given point at that or a later time. This is particularly important for non-perennial rivers, where

a defining characteristic of the dry-wet transition is that the dry initial conditions exacerbate initial losses causing the development of saturated areas and the generation of runoff and streamflow to occur discontinuously throughout the catchment.

Within the context of Mediterranean climate catchments, Gutierrez-Jurado et al. (2019) used an ISSHM in an idealized concept development study to begin exploring the processes leading to the transition from dry streambed to flowing stream. This theoretical study concluded that soil hydraulic properties and unsaturated storage dynamics exhibit strong control over streamflow generation and determine the spatiotemporal development of runoff generating areas and dominant flow generation mechanisms. It also highlighted the importance of understanding the development and progression of active areas (i.e. where processes are active) and their dominant flow generation mechanisms to understand the pathways and threshold of streamflow generation. But how applicable are the findings of this small-scale, idealised and simplified model to real, complex, and larger-scale catchments?

The goal of this study is to investigate the extension of an ISSHM to a mid-sized, ~~real world~~ Mediterranean climate catchment in South Australia with a stream network composed of ephemeral and intermittent reaches. We first present a conceptual model to develop hypotheses of the potential physical flow processes. This conceptual model combines field data with our understanding of the roles of the shallow soils, geology, topography, and water levels in the catchment. Then, we use available shallow soil distribution and hydrological, meteorological, and geologic data in a three-dimensional, HydroGeoSphere (Therrien et al., 2010) model of the catchment, coupled with the Hydraulic Mixing-Cell method (HMC) developed by Partington et al. (2011). The HMC method tracks rainfall as it moves through the catchment, allowing the identification of active areas and the quantification of the contributing flow generation mechanisms on those areas. Given the inherent difficulties of modelling a large, unsaturated domain with contrasting soil layers to capture the physical processes at a rather sudden state change (dry to wet), the goal of this study is not to reproduce the field observations, which in non-perennial rivers are strongly a function of antecedent moisture conditions, but to test and re-evaluate our conceptual understanding of the physical processes occurring in the catchment. ~~Both the insights gained from this modelling process and the challenges encountered in attempting to accurately reproduce the shallow soil distribution, climate, geology, and hydrology of such a dynamic system are discussed.~~

2   Methods

2.1   Study Area

The catchment used for this model is Pedler Creek which is part of the larger Willunga basin located roughly 30 km south of Adelaide, South Australia (Figure 1). Pedler Creek lies within the McLaren Vale region, an area of high agricultural value mainly for the viticulture industry. The catchment area is approximately 107 km^2 and discharges into the sea on the Gulf of St Vincent to the west of the catchment. ~~From the 4 major land uses in the catchment,~~ agriculture (45%-30.4 km^2) and grazing

(46%-31.8km^2) dominate over 90% of the landscape. Urban (residential and commercial) account only for 8% (5.4 km^2), and plantation forestry covers less than 1% (0.38 km^2) of the catchment (Figure 1).

90 A wastewater treatment plant located in the town of McLaren Vale discharges water into the creek; therefore, we only considered the area upstream of the creek before it passes through the town for this study. The Pedler sub-basin has an area of 69 km^2, encompassing over 60% of the catchment and more importantly, it contains roughly 80% of the total length of the stream network. The creek flow regime is intermittent generally from July to September in response to the winter rains and ephemeral during the rest of the year, flowing only after extreme rainfall events. For the period of record 2000-2018 at gauge

95 ID A5030543, the creek flows on average 120 days per year, ranging from 33 to 199 d yr^{-1}. Mean annual discharge is 3.88 x 10^6 m^3 with the higher flows occurring between July and September (Water Data Services, 2019). Mean annual precipitation for the basin is 550 mm ranging from 289 to 812 mm for the period of record 1900-2018 at the McLaren Vale station 232729 (SILO - Australian Climate Data, 2019). Mean daily temperatures range from 37 to 5 °C, with higher daily temperatures occurring in January and lower daily temperatures registered during June and July (SILO - Australian Climate Data, 2019).

100 As part of the Willunga basin, Pedler catchment presents a complex multi-aquifer system. The groundwater system consists of four main aquifers: Quaternary sediments, Port Willunga Formation, the Maslin Sands and the basement fractured rocks (Aldam, 1989). The Maslin Sands and the Port Willunga aquifer are separated in some locations by the Blanch Point Formation which acts as an aquitard. All hydrogeological units outcrop at the surface and regional groundwater flows towards the coast from northeast to southwest.

105 The catchment topography consists of a low-lying coastal plain with mild undulating hills towards the north of the catchment and separated by the Willunga Fault to the steep hills located on the east of the catchment (Figure 2). Elevation ranges from ~400 m on the northeast of the catchment (steep hills) to ~50 m at the catchment's outlet. The hills area on the east of the fault is characterized by having a shallow sediment profile (0.5 - 2 m) which is underlain by the basement rocks while west of the fault the sediments thicken seaward. Surficial soil types (the upper 1.5 m) in the catchment can be clustered into three major

110 soil groups: loam, sand and clay. Covering roughly 62% (42.36 km^2) of the catchment, the loam soils are distributed on the middle-eastern area; sandy soils cover around 32% (21.7 km^2) and are located mainly on the north part of the catchment with some patches present in the middle section (valley); the clay soils account for only 6% (3.94 km^2) of the catchment area and are located on the further downstream section towards the west of the catchment. Most of the stream network (over 80%) is located within the loam soil. Detailed soil profiles obtained from the Department of Environment Water and Natural Resources

115 (DEWNR) consistently show a distinctive clay layer starting from 1.1 to 1.5 meters depth in the sandy soil areas and at around

0.5 m within the loam areas. Despite this general understanding of soil types, there are no available estimates of hydraulic conductivity for these shallow soils.

Surface water-groundwater interactions within Pedler catchment have been documented in previous studies to play a critical role in the creek flow's regime. Sereda and Martin (2000) observed rapid groundwater level rises in response to large precipitation events in some shallow monitoring wells adjacent to creeks while noting that GW level declines in the Quaternary aquifer during 1995-1999 could be attributed to a decrease of yearly precipitation during that period. Moreover, Harrington (2002) observed that groundwater levels seemed to mirror streamflow records for the Creek. While these observations confirm that GW recharge occurs from precipitation and creek seepage, these and other studies have also indicated that GW discharge occurs in some areas of the creek (Harrington 2002, Anders 2012). Further studies have indicated that the creek presents both gaining and losing stream sections, which are not only spatially but temporally variable and which are dependent on rainfall and shallow groundwater levels (Harrington 2002; Brown 2004; Irvine 2016; Anders 2012).

2.2 Conceptual Model of Streamflow Generation Process in Pedler Creek

For medium to large size catchments such as Pedler Creek, the interactions between topographic features such as slope and mean soil thickness, with surficial soil heterogeneity, various aquifers properties, and a spatially variable depth to GW are likely to result in variability in streamflow generation processes developing at different spatiotemporal scales within the catchment. To understand the integrated catchment response as well as the stream network dynamics (development, expansion, and contraction) it is paramount to capture the spatiotemporal occurrence of the different streamflow generation mechanisms. In a similar approach to Gutierrez-Jurado et al. (2019) the streamflow generation mechanisms include: infiltration excess overland flow (IE-OF), saturation excess overland flow (SE-OF), interflow originating from unsaturated or saturated areas (Sat-IF, Unsat-IF) and pre-event groundwater (old GW). Further details on the streamflow generation mechanisms can be found in Gutierrez-Jurado et al. (2019).

Based on field data, available soil and aquifer information and the topography we developed a conceptual model to outline the most likely processes leading to streamflow generation and the resulting dominant streamflow generation for Pedler Creek (Table 1). We identified three major areas with distinctive characteristics: 1) the steep hills on the east, 2) the undulating hills on the north, and 3) the flat valley on the south-west area of the catchment (Figure 3a).

~~The three main areas in the map aim to provide a spatial understanding of the most likely streamflow generating processes.~~ As the ephemeral flows in Pedler Creek occur in direct response to extreme precipitation events (characterized by low-duration, high-intensity precipitation), the temporal component can be considered negligible. Instead, flow is mostly linked to the spatial characteristics of the catchment where we hypothesize that the dominant flow generation mechanism is infiltration excess overland flow originating from the loam and clay soils throughout the catchment. Conversely, it is paramount to include the temporal component to understand how these processes developed and the threshold of flow is reached for intermittent flow during the rainy season. We hypothesize that the dry conditions at the beginning of the rainy season will result in most of the

rainfall to infiltrate due to the high infiltration capacity of the soil. However, differences in topography and soil characteristics will promote different processes to develop as the rainy season progresses. A detailed description of the processes for each area and the spatiotemporal development of the most likely dominant streamflow generation component for intermittent flow is provided below (Figure 3b-d).

2.2.1   Steep Hills; Fast Flow

The steep hills are characterized by a permeable and shallow (top 0.5 m) loam soil underlain by a heavy clay profile with steep slopes (Figure3b). The combination of the shallow loam soil permeability, the high infiltration capacity, and the steep slopes are likely to allow the water to infiltrate and to flow relatively fast as unsaturated-IF towards the stream (Figure 3b.1-2). We hypothesize that the shallow loam soil profile and the water holding capacity of the loam will promote a perched GW mounding along the riverine area which will result in SE-OF from the riverine area and the adjacent hillslope to develop as the dominant streamflow generation mechanism (Figure 3b.3).

2.2.2   Undulating Hills; Slow Flow

The undulating hills consist of a highly permeable deep (top 1.1 m) sandy soil profile underlain by a heavy clay layer with mild slopes (Figure 3.b). The high soil infiltration capacity and permeability of the sand will result in a large infiltration rate allowing most of the precipitation to infiltrate in this area (Figure 3.3.c.4). As the infiltrated water reaches the low permeable clay layer it will move in the subsurface as IF towards the low-gradient areas (Figure 3c.5). We hypothesize that the high infiltration rates in combination with the mild slopes (or low-gradient areas in the valley) will favour the development of a perched GW that will rise uniformly allowing the river to develop into a gaining condition. As the infiltrated water moves as IF it will discharge into the downstream areas (Figure 3c.6). Due to the larger unsaturated storage and the mild slopes, this area will likely take longer to contribute to flow (i.e. more water will be needed and therefore more time to reach the threshold of flow generation). We hypothesize that these areas will provide the "slow flows" necessary to sustain intermittent flow for the days without rainfall during the intermittent season and conversely, they are not likely to contribute to flow during ephemeral events (Figure 3e).

2.2.3   Flat Valley; Mixed Flows

The flat valley comprises a mix of the previous two soil profiles (deep sand and shallow loam underlain by heavy clay) and a heavy clay area, all located in a low-gradient topography (Figure 3d). The GW becomes shallower near the riverine areas in the valley and depth to GW decreases towards the outlet area (the bore with the shallowest GW is located near the outlet where the GW is ~2 m below surface elevation). This zone has the largest draining area with both the steep and undulating hills draining towards it. The diversity of conditions in this area is likely to result in a combination of the processes previously discussed as well as additional ones. We hypothesize that the processes originating on the sandy soil areas on the valley will be similar to those on the undulating hills with the difference that the unsaturated-IF that might originate early during the

season might only contribute with a small amount of flow that might reflect further downstream. We also expect to see some saturated/unsaturated-IF originating early in the season in the loam areas on the valley (Figure 3d.8-9). However, we hypothesize that the low-gradient terrain along with the water holding capacity of the loam soil will slow down water moving as interflow and rather promote the soil saturation to build up in the shallow soil profile. As the saturation increases, we expect the dominant streamflow generation mechanism will switch to saturation excess overland flow from both the hillslope and the river area.

The clay's low permeability will limit infiltration and favour water to pond on the surface on the clay areas, which will eventually result in infiltration excess overland flow (Table 3d.10-11). The large draining area of the valley combined with the low-gradient topography is likely to promote the development of a perched GW along the riverine area which will result in SE-OF along some sections of the river (Figure 3d.9). During wet years, sections of the creek near the outlet where GW is shallow, are likely to develop into a gaining state with old-GW contributing to streamflow (Figure 3d.10). Once the saturation threshold has been met along the riverine area in the steep hills and throughout the loam areas in the valley, SE-OF from those areas and the IE-OF from the clay are likely to contribute with the "fast flows" as travel times for overland flow are generally smaller than those for subsurface processes (Figure 3.b).

2.3   Modelling Platform and HMC Method

To explore the potential for streamflow within the structure of the conceptual model, we built a fully integrated, numerical model of the catchment with the hillslope fraction divided into the three dominant soil types (Figure 4). We used HydroGeoSphere (HGS), a 3-D fully integrated surface-subsurface hydrological model (ISSHM) that allows physically-based simulations of hydrological processes by using the control-volume finite element method to simultaneously solve the surface and subsurface flow equations. The numerical code uses the diffusion wave approximation to the Saint-Venant equations for 2D surface flow and a modified form of the Richards' equation to solve the variably saturated subsurface flow. Further details on the physical and mathematical conceptualisation and the implementation of the HGS code can be found in Aquanty Inc. (2016) and the review by Brunner and Simmons (2012).

The decomposition of flow into the different generation mechanisms is provided by coupling HGS with the HMC method which is based on the modified mixing-cell method (Campana and Simpson, 1984). Using the standard hydrological output from a numerical model, the HMC method allows the partition of flow in any node within the catchment. To do this partition the HMC method tags the existing water at the beginning of the simulation and any new water as it enters the model domain by area of origin (i.e. stream, hillslope, and the porous media), by boundary condition (i.e. the source of water) and for the case of the new water, by the internal model state of saturation of the area of origin (i.e. saturated or unsaturated soil profile). Using these tags, the water is tracked as it moves through the model domain and after each time step of the flow simulation the method calculates the fraction of water in each cell that derives from the different flow components (Table 1). Detailed information on the numerical formulation and application of the HMC method are given in Partington et al. (2011), Partington et al. (2013), and Gutierrez-Jurado et al. (2019).

2.4 Model Setup

2.4.1 Model Discretization

The topography for the surface elevation was implemented by using a digital elevation model (DEM) with 5 m contours and
215   a final resolution of 10 m. After testing several potential nodal spacing options (see Supplemental Information for a description
of this process) the final 2D surface domain discretisation consisted of 3015 nodes and 5869 triangles with nodal spacing
ranging from ~40-70 m around the streams and up to ~500 m at the catchment boundary. Vertically, the subsurface domain
was discretised into 28 layers (Figure 4). For layers 1-2 the resolution was 0.05 m, followed by 0.2 m in layers 3-13 (up to a
depth of 2.1 m), grading to 5 m in layers 14-18 (a depth of 20 meters) and 12 to 120 m at the bottom of the domain in layers
220   19-28. The final 3D grid consisted of 84,420 total nodes and 159,192 total triangular elements. As the streams in the study
area were only a few metres wide the DEM did not capture the incision of the streams into the landscape. In order to overcome
this limitation, the digital elevation model was post-processed using a Python routine to depress the elevation of the stream
nodes.

2.4.2 Porous Media Properties

225   Hydraulic conductivity, porosity and specific storage based on literature estimates for the Quaternary Sediments, Port Willunga
Formation, Blanche Point formation and the Maslin Sands were assigned using rasters of the top and bottom elevations for
each unit (Aldam 1990; Anders 2012; Irvine 2016; Martin 1998, 2006) (Table 2). Unsaturated hydraulic parameters were then
estimated from Carsel and Parrish (1988) and Mirus et al. (2011), which had the closest hydraulic conductivity values to the
estimates for each hydrogeological unit. The basement fracture rock formation is believed to act as an impervious layer
230   throughout most of their length (Knowles et al., 2007; Martin, 1998); therefore, the elements for this layer were assumed to be
inactive on the time-scale of these simulations.

The shallow soils were considered as the top 1.5 m of the subsurface domain which was the average depth reported in the soil
characterisation datasheets. The information of the horizontal and vertical distribution of soils was assigned into the model
using 2D overlays (horizontal) for the three main soil areas and the mesh layers generated during the grid discretization
235   (vertical). We used a digital soil-landscape map obtained from the Department for Environment, Water and Natural Resources
of South Australia (DWLBC, 2004; Hall et al., 2009) to differentiate the spatial distribution of the three dominant shallow soil
types. The vertical heterogeneity was determined by analysing soil characterisation datasheets from detailed soil profiles
available within the Pedler sub-catchment [DEWNR 2016]).

Data of particle size distribution at different depths (soil layers) from six soil profiles (two within the Pedler sub-catchment
240   and four nearby) were used to estimate soil hydraulic parameters for the three dominant soil types in the catchment. We used
the ROSETTA model H2 (Schaap et al., 2002) to select a range of values typical of each soil type to be tested. As explained
below, the influence of the hydraulic conductivity values for each shallow soil, which is typically highly variable and not well
known at catchment scale, was then explored using scenarios.

2.4.3 Overland Flow Properties

Manning's roughness coefficients (n) derived from Chow (1959) were implemented for the three prevalent land uses (i.e. agricultural, pasture and urban) which account for over 99.5% of the catchment area. We used the values for cultivated areas with mature row crops (4.05E-7 $d/m^{1/3}$) for the agricultural areas, for pasture with no bush and short grass (3.47E-7 $d/m^{1/3}$), and the value of asphalt (1.85E-7 $d/m^{1/3}$) was applied to the urban area (Table 2). For the stream network, we used values for a clean and straight natural channel for the headwater sections (4.05E-7 $d/m^{1/3}$) and of weedy reaches for the middle-lower sections (1.15E-6 $d/m^{1/3}$). Rill storage height was set to 0.01 m uniformly across the domain and no obstruction storage height was implemented. The coupling length was set at 0.001 to warrant a good coupling of the surface-subsurface domains which is paramount to capture streamflow generation processes (Liggett et al., 2014).

2.4.4 Simulation Period and Initial Conditions

We selected a 4-year simulation period from January 2015 to December 2018 to ensure a representative set of years with average (2017 ~500 mm/y), below average (2015 and 2018 ~400 mm/y) and above-average (2016 ~800 mm/y) annual rainfall amounts. Precipitation records from the McLaren Vale (located in the valley) and the McLaren Flat (located near the steep hills) stations (MEA, 2019) were averaged and applied as a fluid flux to the surface of the model domain. To determine the optimal time resolution for the precipitation forcing we tested preliminary models with quarterly-hour, 1-hour and 24-hour inputs. Results from the preliminary models show better convergence and smaller errors in the water balance for the hourly precipitation inputs. Estimates of potential evapotranspiration (ET_0) were only available at a daily time step; therefore, we used values of solar radiation to approximate ET_0 at hourly intervals to match the precipitation inputs. Values of ET_0 that were less than 0.0001 m/h were considered numerical noise and were excluded from the input dataset. The resulting ET_0 dataset was applied to the surface domain. Actual evapotranspiration (ET) and interception are simulated as mechanistic processes within HGS using the concepts by Kristensen and Jensen (1975) and Wigmosta et al. (1994) which require plant and soil conditions (Aquanty, 2016). Vegetation characteristics cited in the literature for Eucalyptus were used on the riverine area and values typical of grass (Banks et al., 2011; Geeroms 2009; Hingston et al., 1997) were used for the rest of the catchment (Table 2). Although a large area on the catchment consists of vineyards, during the winter months the vines are dormant without leaves and grass is commonly used as an inter-row soil cover. We did not include the effects of irrigation, ET, and interception during the vines growing season as we considered the overall effects for streamflow generation would be negligible since they occur during the driest and hottest months of the year when the stream network is dry. With the simulation starting in January (the hottest month) we assumed completely dry initial conditions for the surface domain.

Initial groundwater levels were iteratively achieved by draining a fully saturated model and comparing the resulting water table to field data. The goal was to obtain realistic soil moisture profiles characteristic of dry, summer conditions and a smoothly varying water table surface. The resulting water levels were compared with the long-term average of data obtained from the Government of South Australia (https://www.waterconnect.sa.gov.au/) for the McLaren Vale prescribed wells area.

Preference was given to matching wells with shallow GW heads (< 10 m depth) located on the flat valley area and close to streams, which are known to transition from losing to gaining conditions in response to increases in the groundwater level. Finally, an output time where the simulated GW heads at four of the five wells in this area were within 1 m of average recorded levels was selected as the initial conditions for the porous media in the subsequent simulations. Initial groundwater levels in the steep hills area matched average recorded levels within 1 – 28 m, where the depth to water is quite deep and varies by tens of meters across the fault line (Figure 4).

2.4.5   Boundary Conditions

Boundary conditions for the outflow in the surface domain were set as a critical-depth boundary at the catchment's outlet and as a no-flow boundary condition for the rest of the domain. We applied a fluid transfer boundary condition around the catchment outlet which allows for the discharge of groundwater through the subsurface. The hydraulic gradient for the fluid transfer was given by setting a hydraulic head ~4 m below the surface elevation (the known deepest GW head near the outlet) at 10 m from the outlet faces.

2.4.6   Simulation Implementation and Data Post-processing

The simulations were performed in HGS using the control-volume finite-element mode and the dual-node approach for surface-subsurface coupling. We used an adaptive time step with a computed under-relaxation factor scheme to aid the computational efforts. Adaptive time-stepping was applied by an initial step size of 0.001 days, a maximum step multiplier factor of 2.0, and a maximum time-step of 5 days. The simulations were run in parallel mode using 6 CPUs to partition the model domain. The HMC method was set up to track the flow generation mechanisms originating from the different soils in the overland areas (clay, loam, and sand), directly in the river, and from the porous media (Table 1).

We ran over 52 preliminary models testing different mesh discretisations and time resolutions for the model forcings (i.e. precipitation and ET), simulation control values, and draining simulations to try to select the optimal model setup. From the final setup, we developed a final set consisting of 8 scenarios to be tested; four corresponding to sets with different combinations for the shallow soils hydraulic properties (K_{sat} and their corresponding unsaturated storage parameters α, β, and θr); and four scenarios with different values for incising the river nodes (Table 3). Due to the computational constraints, only one set of soil hydraulic properties was used to test the scenarios with the incised stream. Results from these two sets of scenarios were used to evaluate the need to modify and test further scenarios.

Model output for the surface domain (2D) was post-processed to identify and quantify the activation of areas (flow onset) and the flow generation mechanisms. The output files were processed in Python to determine the HMC fraction (flow generation mechanism) that contributed most of the flow (dominant fraction) at every single node and for each output time. Results of the dominant fraction were then included as a new variable to the overland output file. A water depth threshold equal to the rill storage height (0.01 m) was used to determine when an area was considered active (i.e. values of 0.01 m or less were considered as rill storage and not flow). Output for the porous media (3D) was used to support the HMC dominant fractions findings.

3   Results

The computational demands of modelling a large and variably saturated domain subject to sudden state changes from dry to wet conditions led to in extremely slow model convergence. From the set of scenarios testing different values for incising the stream (Table 3), only scenario 8 (incision = 10m) finished under a reasonable computation timeframe. Scenarios 5-7 showed less than 10% of progress after 20 days of computation time. Nevertheless, the comparable results between scenario 8 and 4 which shared the same soil hydraulic properties but had the two ends of the spectrum in respect to the river incision (the most vs. none) suggest that results from scenarios 5-7 would have likely shown similar results. Therefore, from here on we will only focus on the results from scenarios 1-4 (different soil hydraulic properties) and 8 (river incised).

3.1   Active Areas and Dominant Flow Generation Processes Determined with HMC

The development of active areas (initiation of flow) in terms of the timing and extent was similar among scenarios 1-4, while for scenario 8 (scenario with the incised stream nodes) the aerial extent was consistently smaller (Figure 5). Across all scenarios, flow was generated first on areas from the steep hills and these areas expanded and contracted throughout the simulation. Fragmented active areas developed along the stream network for scenario 8 while for scenarios 1-4, the active areas along the stream developed as result of the flow from the hills connecting to stream network and expanding from there. Although the overall active areas along the river were larger for scenarios 1-4, a larger length of the stream network showed flow for scenario 8.

The development of active areas across scenarios matched the areas where the shallow soil profile reached saturation. The dominant flow generation mechanism on most of the steep hills shifted from IE-OF from the loam soil in the hill slopes during precipitation events to pre-event GW afterwards. A few small areas on the steep hills also showed unsaturated-IF as the dominant mechanism. In the area near the outlet the flow generation mechanisms during precipitation events included IE-OF from the clay hillslopes, in-stream unsaturated-IF, and pre-event GW. After precipitation events pre-event GW was prevalent on the areas near the outlet. The flow simulated in the few areas along the stream network close to the sandy areas from the mild hills simulated flow mostly through unsaturated-IF.

3.2   Water Balance Comparisons

Among the scenarios with different sets of hydraulic properties (scenarios 1 through 4), the water balance breakdown was virtually identical for scenarios 2 & 3 (<0.1%) and 1 & 4 (~0.1%) and only small differences (as a percentage of the overall water balance) were observed between scenarios 2 & 3 and 1 & 4 (~0.1 - 4%) (Figure 6; also see Supplemental Information for a full breakdown of the water balance results). The results showed a higher porous media (PM) and overland flow (OLF) flux component and a smaller fluid transfer (FT) flux component for scenarios 2 & 3 than for scenarios 1 & 4. Since the change in storage is the sum of the OLF and PM components, scenarios 2&3 also showed a larger change in storage than scenarios

1&4. The largest differences in the water balance were simulated between scenarios 1-4 (no incised stream) and scenario 8 (incised stream). Scenario 8 had the largest OLF flux and change in storage and the smaller ET flux.

4   Discussion

The goals of this study were to provide insight into streamflow generation processes at the catchment scale for an intermittent, Mediterranean climate catchment to better understand the importance of controlling characteristics identified previously with small-scale theoretical models. In particular, the role of soil heterogeneity on different streamflow generation processes has been documented in previous studies. For instance, studies have shown that vertical soil heterogeneity can result in the development of perched saturated zones that contribute to flow generation (Hathaway et al., 2002; Maxwell and Kollet, 2008). Other studies indicated that horizontal heterogeneity contributed to the spatio-temporal variability of flow generation under different mechanisms which overall resulted in longer flow durations due to delays in runoff occurring from areas with high infiltration capacities (Ebel et al., 2016; Luce & Cundy, 1994; Smith & Hebbert, 1979). Therefore, in this study we developed a conceptual framework of the hydrological processes identified in three distinct subregions of the Pedler Creek catchment. In consideration of the findings of Gutierrez-Jurado et al. (2019), this conceptualisation further suggested flow generation mechanisms across the catchment corresponding to vertical and longitudinal heterogeneity of the shallow soils, catchment topography, and SW-GW interactions near the outlet. The steep hills are characterised by permeable shallow loam soils, steep slopes and deep GW heads which would result in sat-IF and SE-OF. The undulating hills are characterised by high permeable deep sandy soils, mild slopes and deep GW heads which would result in unsat-IF. The flat valley consisted of a mix of the previous soils with the addition of a clay area all located in low-gradient terrain and presenting the areas of shallow GW heads which would result in a mix of flow generation processes. A final set of 8 models comprising 4 scenarios testing different sets of soil hydraulic properties for the shallow soils and 4 scenarios testing different values for incising the stream nodes were tested.

Model results overall supported our conceptual understanding of the flow generating processes in Pedler Creek. Results from the active areas showed distinct mechanism developing in the three major areas (Figure 5), supporting the idea that there is a spatial variation of flow generation processes in Pedler Creek. In the model, flow developed first at the steep hills areas (fast-flow) and the dominant mechanism was SE-OF with a few areas showing unsat-IF as hypothesized in our conceptual model (Figures 3b and 5). An unexpected development was the contribution of pre-event GW during flow recessions. In this area the pre-event GW was likely to be pre-event soil water since evaluation of the model showed that the groundwater level did not rise to intersect land surface in this area. The flows generated in the valley near the outlet were similarly simulated via the conceptualized mechanisms (Figures 3d and 5). We saw small areas with flow originating from IE-OF from the clay areas, and a combination of unsat-IF and pre-event GW for the rest of the active areas in this region. The GW did rise above the surface elevation in this area, supporting the GW contribution to flow in this area. Finally, in the few small areas close to the sandy undulating hills region, flow was simulated through the unsat-IF mechanism as predicted in our conceptual framework

370 (Figures 3c and 5). These results support the findings by Gutierrez-Jurado et al. (2019) who suggested that soil properties largely dictate the dominant flow generation mechanisms and that unsaturated storage dynamics control the thresholds and pathways of flow. The development and extent of active areas and the dominant flow generation mechanisms estimated by the HMC method and the water balance results were almost identical for scenarios 1-4, indicating that knowledge of the exact hydraulic conductivity value of a given soil type is less importance than capturing the general vertical and longitudinal soil

375 heterogeneity across the catchment. The small differences simulated between scenarios 2 & 3 and 1 & 4 show that the models were more sensitive to variations on the hydraulic properties of the loam soil as the scenarios with identical responses (2 & 3 and 1 & 4) shared the same loam but different sand hydraulic properties. The loam's smaller hydraulic conductivity for scenarios 2 & 3 (0.0624 m^3/d) limited infiltration, which translated to more OLF. At the same time, the higher water holding capacity in the loam areas might have resulted in slower subsurface flows to either exfiltrate to the surface or to contribute to

380 the fluid transfer (FT) through the subsurface boundary. In contrast, both tested values for the sand resulted in a low water holding capacity that allowed the incoming precipitation to drain past the root zone and move in the subsurface contributing to the FT. This is supported by the higher FT values shown for scenarios 1&4 (Figure 6).

The greatest differences for both the water balance and HMC results among the tested scenarios were caused by differences in stream definition between scenarios 1-4 (no incised stream) and scenario 8 (incised stream). The effects of the incised stream

385 in scenario 8 resulted in a larger OLF flux, a smaller ET flux, and in an overall smaller extent of active areas (Figure 5 and supplemental information). The roles of a good channel representation in ISSHMs is extensively discussed by Käser et al. (2014). While their discussion of channel representation revolves on the ability of ISSHMs to quantify GW-stream interactions (which was not a major component for this model), the hydrological principles are relevant and transferable to explain the importance of channel representation to capture streamflow generation processes. Without a defined channel, the connection

390 to the Pedler Creek floodplain was lost and the shallow sheet-flow and most of the precipitation infiltrated and stayed within the porous media. The importance of the connection of the floodplain to the channel is also discussed by Käser et al. (2014), as they argued that not only is the channel topography important but also its connection to the floodplain given that riverbank geometry is key for bank storage and overbank flooding. Although overbank flooding is not considered important for this study (flows in Pedler only rarely will experience overbank flooding), the stream-floodplain connectivity and bank storage

395 were key aspects under our model conceptualisation. Namely, the predicted dominant mechanisms relied upon either the saturation to build up along the riverine zone in the loamy areas which would lead to saturation excess overland flow; and we expected a perched groundwater developing on the sandy hillslopes which would, after intersecting the stream, contribute with interflow into the stream. While we observed these processes developed, they only occurred briefly as very shallow runoff. Another important consideration for the channel representation in streamflow generation studies for non-perennial streams is

400 the relationship between flow and the wetted area. The larger the channel (both vertically and horizontally), the larger the area of exchange to the unsaturated zones during a flow event (Doble et al., 2012), which would be exacerbated under low flows (Käser et al., 2014). This is particularly significant when evaluating streamflow generation for non-perennial streams where high streambed infiltration and transmission losses are common (Gutierrez-Jurado et al., 2019; Levick et al., 2008; Shanafield

& Cook, 2014; Snelder et al., 2013) and often prevent flows from even reaching the catchment outlet (Keppel & Renard, 1962; Aldridge, 1970). In this study, we observed that without a defined stream to 'channel' the water, the little overland flow that was simulated in scenarios 1-4 (no incised stream) spread over a larger area than in scenario 8 where the stream was incised (Figure 5). The same was true for the patterns of increased saturation of the porous media across the catchment (Figure 6). Results from the water balance reflected the effects of having both flows and porous media saturation spread over larger areas by exacerbating ET and decreasing the overall amount of overland flow for scenarios 1-4 (Supplemental Information). This is consistent with the remarks by Käser et al. (2014) regarding the likely impacts to the water flow budget by the spatio-temporal aspects linked to channel representation due to spatial exchange patterns.

Finally, this study highlighted both the need for further studies examining streamflow generation processes in additional non-perennial catchments and the inherent challenges associated with capturing unsaturated zone dynamics at catchment scale. Indeed, modelling this non-perennial river system confirmed the inherent difficulties of using ISSHMs in medium size non-perennial river catchments and reiterated why so few studies have been done on this topic. Extensive work was needed to set up this model, and the large computational time to run the simulations was a major constraint to both establishing initial conditions and exploring scenarios. For example, when draining the model, simulations running for over 10 days only progressed to day 100 of the simulation. Relaxing the mesh allowed us to develop reasonable initial conditions after testing over 37 scenarios. For the scenarios running for the full 4-year simulation, simulation convergence consistently slowed down when the simulation encounter a precipitation input and particularly during prolonged precipitation events (i.e. consecutive precipitation inputs), which is expected given the highly non-linear equations for unsaturated flow in the unsaturated surface domain. Despite the conceptual advantages of using a fully physically-based model to explicitly capture all surface and groundwater processes, future studies may try to identify a suitable simplified surrogate model to speed up simulations and focus on specific areas where particular streamflow generation processes are thought to be dominant.

5   Conclusion

There are hundreds of similar non-perennial river systems in the semi-arid, coastal Mediterranean climate regions of South and Western Australia, California, South Africa, and around the Mediterranean itself. This study provides an initial step towards understanding non-perennial streamflow generation processes at the catchment scale and provides a template for using ISSHM's for process understanding in these stream systems. The development of a conceptual model of the most important factors impacting flow generation processes within Pedler catchment presented a hypothesis that combined our understanding of field data with lessons learned from previous studies. This conceptualization was key to inform the model setup and to capture dynamics of streamflow generation in this non-perennial stream system. Difficulties in setting up and running the model reaffirmed the numerical difficulties experienced in large scale unsaturated models, as accurately reproducing the topography and observed initial conditions was a challenge and model runtimes prohibited extensive exploration of multiple scenarios. In particular, the importance of preserving channel representation to model streamflow generation on non-perennial

systems became apparent in the scenarios. Yet overall the model results confirmed our conceptual understanding that soil type, unsaturated storage dynamics and topography are major controls for streamflow generation processes in non-perennial streams. The similarity in the results from scenarios comparing soil hydraulic properties across the literature range for each soil type showed that exact knowledge of these values for a given soil type is not critical for identifying streamflow generation processes

440   if the conceptual model is accurate and the vertical and longitudinal soil heterogeneity is captured. Given that soil properties are often highly heterogeneous within a catchment and rarely well-known, this result is will be important to future modelling studies.

Code/Data Availability

The data for this model were sourced through publicly available resources as cited in the methods. Commercially available

445   AlgoMesh (HydroAlgorithmics) software and HydroGeoSphere (Aquanty) software was used to prepare and run model simulations. Post-processing routines and model files are currently in the process of being archived by Flinders University.

Competing Interests

The authors declare they have no competing interests.

Author Contribution

450   KGJ, MS, and DP conceived the project design. KGJ developed the conceptual model. KGJ developed the numerical model with assistance from DP. KGJ and MS prepared the manuscript with contributions from all co-authors.

Acknowledgements

This research was funded by a Discovery Early Career Research Award from the Australian Research Council (DE150100302).

References

455   Aldam, R.G.: Willunga Basin hydrogeological investigations 1986/88. South Australia Department of Mines and Energy. Report Book, 89/22, 1989.

Aldam, R. G.: Willunga Basin Groundwater Investigation Summary Report. Groundwater and Engineering, Department of Mines and Energy, Government of South Australia. Report Book, 90/71, 1990.

Aldridge, B. N.: Floods of November 1965 to January 1966 in the Gila River basin, Arizona and New Mexico, and adjacent

460   basins in Arizona. US Geological Survey Water-Supply Paper 1850-C, 176 p. https://doi.org/10.3133/wsp1850C, 1970.

Ambroise, B.: Variable 'active' versus 'contributing' areas or periods: A necessary distinction. Hydrological Processes, 18, 1149–1155. https://doi.org/10.1002/hyp.5536, 2004.

Anders, L.: Surface - Water and Groundwater Interactions Along Pedler Creek, 2012.

Anderson, M. P., Woessner, W. W., and Hunt, R. J.: Applied groundwater modeling: simulation of flow and advective transport. Academic press (second edition), 2015.

Aquanty: HydroGeoSPhere user manual, Release 1.0. Waterloo, Ontario, Canada: Aquanty Inc, 2016.

Banks, E. W., Brunner, P., & Simmons, C. T.: Vegetation controls on variably saturated processes between surface water and groundwater and their impact on the state of connection. Water Resources Research, 47(11), 1–14. https://doi.org/10.1029/2011WR010544, 2011.

Beven, K.: Runoff generation in semi-arid areas, in Dryland Rivers: Hydrology and geomorphology, edited by Bull and M. J. Kirkby, John Wiley & Sons, Ltd., 2002.

Boulton, A. J., Rolls, R. J., Jaeger, K. L., & Datry, T.: Hydrological connectivity in intermittent rivers and ephemeral streams. In Intermittent rivers and ephemeral streams (pp. 79-108). Academic Press, 2017.

Brown, K. G. (2004). Groundwater contributions to streamflow along Willunga Fault, McLaren Vale, South Australia.

Brunner, P., and Simmons, C. T.: HydroGeoSphere: A fully integrated, physically based hydrological model. Ground Water, 50(2), 170–176. https://doi.org/10.1111/j.17456584.2011. 00882.x, 2012.

Campana, M. E., and Simpson, E. S.: Groundwater residence times and recharge rates using a discrete-state compartment model and 14C data. Journal of Hydrology, 72, 171–185. https://doi.org/10.1016 /0022-1694(84)90190-2, 1984.

Carr, A. E., Loague, K. and VanderKwaak, J. E.: Hydrologic-response simulations for the North Fork of Caspar Creek: Second-growth, clear-cut, new-growth, and cumulative watershed effect scenarios. Hydrological Processes, 28(3), 1476–1494. https://doi.org/10.1002/hyp.9697, 2014.

Chow, V. T.: Open channel hydraulics (p. 680). New York: McGraw-Hill, 1959.

Costigan, Katie H., Kennard, Mark J., Leigh, Catherine, Sauquet, Eric, Datry, Thibault, Boulton, A. J.: Flow regimes in intermittent river and ephemeral streams., in Intermittent Rivers: Ecology and Management., edited by A. J. Datry, Thibault; Bonada, Nuria; Boulton, p. 300., 2017.

Cudennec, C., Leduc, C. and Koutsoyiannis, D.: Dryland hydrology in Mediterranean regions - A review, Hydrol. Sci. J., 52(6), 1077–1087, doi:10.1623/hysj.52.6.1077, 2007.

DEWNR, Soil and Land Program: Soil Characterisation Sites. Retrieved on: 10 June 2018 from: https://data.sa.gov.au/data/dataset/soil-characterisation-sites, 2016.

Di Giammarco, P., Todini, E., and Lamberti, P.: A conservative finite elements approach to overland flow: The control volume finite element formulation. Journal of Hydrology, 175(1–4), 267–291. https://doi.org/10.1016/S0022-1694(96)80014-X, 1996.

Doble, R., Brunner, P., McCallum, J., and Cook, P. G.: An analysis of river bank slope and unsaturated flow effects on bank storage. Groundwater, 50(1), 77-86. https://doi:10.1111j.1745-6584.2011.00821.x, 2012.

DWLBC.: Soils (soil type). Department for Environment and Water. Retrieved on: 10 June 2018 from: https://data.sa.gov.au/data/dataset/soil-type, 2016.

Ebel, B. A., Rengers, F. K., & Tucker, G. E.: Observed and simulated hydrologic response for a first-order catchment during extreme rainfall 3 years after wildfire disturbance. Water Resources Research, 52, 9367–9389. https://doi.org/10.1002/2016WR019110, 2016.

Fekete, B. M. and Vörösmarty, C. J.: The current status of global river discharge monitoring and potential new technologies complementing traditional discharge measurements, IAHS Publ., 2002.

Geeroms, J.: 3D modeling to evaluate infiltration furrows for rainwater harvesting in the semiarid zone of Chile. Thesis at the Department of Soil Management. Ghent University, Belgium, 110 pp, 2009.

Geiger, R.: Überarbeitete Neuausgabe: Köppen-Geiger/Klima der Erde, 1961.

Gutierrez-Jurado, K. Y., Partington, D., Batelaan, O., Cook, P. and Shanafield, M.: What triggers streamflow for Intermittent Rivers and Ephemeral Streams in Low-Gradient Catchments in Mediterranean Climates, Water Resour. Res., 55, 9926–9946, doi:10.1029/2019WR025041, 2019.

Hall, J. A. S., Maschmedt, D. J., and Billing, B.: The soils of southern South Australia. Department of Water, Land and Biodiversity Conservation, Government of South Australia, 2009.

Harrington, G. A.: Recharge mechanisms to Quaternary sand aquifers in the Willunga Basin, South Australia, 2002.

Hathaway, D.L., Ha, T.S., and Hobson, A.: Transient Riparian Aquifer and Stream Exchanges along the San Joaquin Stream. In Proceedings of the Ground Water/Surface Water Interactions, AWRA 2002 Summer Specialty Conference, July 1-3, 2002, Colorado, 169-174, 2002.

Heppner, C. S., Loague, K. and VanderKwaak, J. E.: Long-term InHM simulations of hydrologic response and sediment transport for the R-5 catchment, Earth Surf. Process. Landforms, 32, 1273–1292, doi:10.1002/esp.1474, 2007.

Hingston, F.J., Galbraith, J.H., and Dimmock, G.M.: Application of the process-based model BIOMASS to Eucalyptus globules subsp. Globules plantations on ex-farmland in south Western Australia: I. Water use by trees and assessing risk of losses due to drought. Forest Ecology and Management, 106, 141-156, 1997.

Irvine, M. L.: Using tracers to determine groundwater fluxes in a coastal aquitard-aquifer system, Flinders University., 2016.

Käser, D., Graf, T., Cochand, F., Mclaren, R., Therrien, R. and Brunner, P.: Channel Representation in Physically Based Models Coupling Groundwater and Surface Water: Pitfalls and How to Avoid Them, Groundwater, 52(6), 827–836, doi:10.1111/gwat.12143, 2014.

Keppel, R. V., and Renard, K. G.: Transmission losses in ephemeral stream beds. Journal of the Hydraulics Division, 88(3), 59-68, 1962.

Knowles, I., Teubner, M., Yan, A., Rasser, P., & Lee, J. W.: Inverse groundwater modelling in the Willunga Basin, South Australia. Hydrogeology Journal, 15(6), 1107–1118, doi:10.1007/s10040-007-0189-6, 2007.

Kollet, S., Sulis, M., Maxwell, R. M., Paniconi, C., Putti, M., Bertoldi, G., Coon, E. T., Cordano, E., Endrizzi, S., Kikinzon, E., Mouche, E., Mügler, C., Park, Y. J., Refsgaard, J. C., Stisen, S. and Sudicky, E.: The integrated hydrologic model

intercomparison project, IH-MIP2: A second set of benchmark results to diagnose integrated hydrology and feedbacks, Water Resour. Res., 53(1), 867–890, doi:10.1002/2016WR019191, 2017.

530   Kristensen, K. J., and Jensen, S. E.: A model for estimating actual evapotranspiration from potential evapotranspiration. Hydrology Research, 6(3), 170-188. https://doi.org/10.2166/nh.1975.0012, 1975.

Levick, L. R., Goodrich, D. C., Hernandez, M., Fonseca, J., Semmens, D. J., Stromberg, J., et al.: The ecological and hydrological significance of ephemeral and intermittent streams in the arid and semi-arid American Southwest. U.S. Environmental Protection Agency and USDA/ARS Southwest Watershed Research Center. EPA/600/R-08/134, ARS/233046,

535   2008.

Liggett, J. E., Werner, A. D., Smerdon, B. D., Partington, D. and Simmons, C. T.: Fully integrated modeling of surface-subsurface solute transport and the effect of dispersion in tracer hydrograph separation, Water Resour. Res., 50(10), doi:10.1002/2013WR015040, 2014.

Luce, C. H., and Cundy, T. W.: Parameter identification for a runoff model for forest roads. Water Resources Research, 30(4),

540   1057–1069. https://doi.org/10.1029/93WR03348, 1994.

Martin, R. R.: Report Book 98/28 Willunga Basin - Status of Groundwater Resources 1998. P. I. a. R. SA. Adelaide, South Australia., 1998.

Martin, R. R.: Hydrogeology and Numercial Groundwater Flow Model for the McLaren Vale Prescribed Wells Area Summary Report, REM, Adelaide and Mount Lofty Ranges Natural Resource Management Board., 2006.

545   Maxwell, R. M., & Kollet, S. J.: Quantifying the effects of three-dimensional subsurface heterogeneity on Hortonian runoff processes using a coupled numerical, stochastic approach. Advances in Water Resources, 31(5), 807–817. https://doi.org/10.1016/j.advwatres.2008. 01.020, 2008.

Merheb, M., Moussa, R., Abdallah, C., Colin, F., Perrin, C. and Baghdadi, N.: Hydrological response characteristics of Mediterranean catchments at different time scales: a meta-analysis, Hydrol. Sci. J., 61(14), 2520–2539,

550   doi:10.1080/02626667.2016.1140174, 2016.

Milly, P. C. D., Dunne, K. A. and Vecchia, A. V.: Global pattern of trends in streamflow and water availability in a changing climate, Nature, 438(7066), 347–350, doi:10.1038/nature04312, 2005.

Mirus, B. B., Loague, K., VanderKwaak, J. E., Kampf, S. K. and Burges, S. J.: A hypothetical reality of Tarrawarra-like hydrologic response, Hydrol. Process., 23, 1093–1103, doi:10.1002/hyp.7241 A, 2009.

555   Mirus, B. B., Loague, K., Cristea, N. C., Burges, S. J. and Kampf, S. K.: A synthetic hydrologic-response dataset, , 3692(January), 3688–3692, doi:10.1002/hyp.8185, 2011.

Mirus, B. B., Ebel, B. A., Heppner, C. S., and Loague, K.: Assessing the detail needed to capture rainfall-runoff dynamics with physics based hydrologic response simulation. Water Resources Research, 47, 1–18. https://doi.org/10.1029/2010WR009906 W00H10, 2011.

560   Mirus, B. B., and Loague, K.: How runoff begins (and ends): Characterizing hydrologic response at the catchment scale. Water Resources Research, 49, 2987–3006. https://doi.org/10.1002/wrcr.20218, 2013.

Panday, S. and Huyakorn, P. S.: A fully coupled physically-based spatially-distributed model for evaluating surface / subsurface flow, , 27, 361–382, doi:10.1016/j.advwatres.2004.02.016, 2004.

Partington, D., Brunner, P., Simmons, C. T., Therrien, R., Werner, A. D., Dandy, G. C. and Maier, H. R.: A hydraulic mixing-cell method to quantify the groundwater component of stream flow within spatially distributed fully integrated surface water-groundwater flow models, Environ. Model. Softw., 26(7), 886–898, doi:10.1016/j.envsoft.2011.02.007, 2011.

Partington, D., Brunner, P., Frei, S., Simmons, C. T., Werner, A. D., Therrien, R., Maier, H. R., Dandy, G. C. and Fleckenstein, J. H.: Interpreting streamflow generation mechanisms from integrated surface-subsurface flow models of a riparian wetland and catchment, Water Resour. Res., 49(9), 5501–5519, doi:10.1002/wrcr.20405, 2013.

Pierini, N. A., Vivoni, E. R., Robles-Morua, A., Scott, R. L., & Nearing, M. A.: Using observations and a distributed hydrologic model to explore runoff thresholds linked with mesquite encroachment in the Sonoran Desert. Water Resources Research, 50, 8191–8215. https://doi.org/10.1002/2014WR015781, 2014.

Poff, N. L. R., Bledsoe, B. P. and Cuhaciyan, C. O.: Hydrologic variation with land use across the contiguous United States: Geomorphic and ecological consequences for stream ecosystems, Geomorphology, 79(3–4), 264–285, doi:10.1016/j.geomorph.2006.06.032, 2006.

Schaap, M. G., Leij, F. J. and van Genuchten, M. T.: ROSETTA: a computer program for estimating soil hydraulic parameters with hierarchical pedotransfer functions, J. Hydrol., 251(3–4), 163–176, doi:https://doi.org/10.1016/S0022-1694(01)00466-8., 2002.

Sereda, A. and Martin, R. R.: Willunga groundwater basin observation well network monitoring and trends in aquifers, 2000.

Shanafield, M., & Cook, P. G.: Transmission losses, infiltration and groundwater recharge through ephemeral and intermittent streambeds: A review of applied methods. Journal of Hydrology, 511, 518–529. https://doi.org/10.1016/j.jhydrol.2014.01.068, 2014.

Shanafield, M., Bourke, S., Zimmer, M. and Costigan, K.: Overview of the hydrology of non-perennial rivers and streams, Wiley Interdiscip. Rev. Water., 2000.

Shangguan, W., Hengl, T., Mendes de Jesus, J., Yuan, H., & Dai, Y.: Mapping the global depth to bedrock for land surface modeling. Journal of Advances in Modeling Earth Systems, 9, 65–88. https://doi.org/10.1002/2016MS000686, 2017.

Sheldon, F., Bunn, S. E., Hughes, J. M., Arthington, A. H., Balcombe, S. R., & Fellows, C. S.: Ecological roles and threats to aquatic refugia in arid landscapes: Dryland river waterholes. Marine and Freshwater Research, 61(8), 885–895. https://doi.org/10.1071/ MF09239, 2010.

SILO, Australian Climate Data.: Station 232729 climate records. Retrieved March 28, 2019, from https://www.longpaddock.qld.gov.au/silo/, 2019.

Skoulikidis, N. T., Sabater, S., Datry, T., Morais, M. M., Buffagni, A., Dörflinger, G., et al.: Non-perennial Mediterranean Rivers in Europe: Status, pressures, and challenges for research and management. Science of the Total Environment, 577, 1–18. https://doi.org/10.1016/ j.scitotenv.2016.10.147, 2017.

595   Smith, R. E., & Hebbert, R. H. B.: A Monte Carlo analysis of the hydrologic effects of spatial variability of infiltration. Water Resources Research, 15(2), 419–429. https://doi.org/10.1029/WR015i002p00419, 1979.

Snelder, T. H., Datry, T., Lamouroux, N., Larned, S. T., Sauquet, E., Pella, H., & Catalogne, C.: Regionalization of patterns of flow intermittence from gauging station records. Hydrology and Earth System Sciences, 17(7), 2685–2699. https://doi.org/10.5194/hess-17-2685-2013, 2013.

600   Sophocleous, M.: Interactions between groundwater and surface water: The state of the science. Hydrogeology Journal, 10(1), 52–67. https://doi.org/10.1007/s10040-001-0170-8, 2002.

Therrien, R., McLaren, R.G., Sudicky, E.A., Panday, S.M.: HydroGeoSphere: A three-dimensional numerical model describing fully-integrated subsurface and surface flow and solute transport. Groundwater Simulations Group, Waterloo, Ont., Canada, 2010.

605   VanderKwaak, J. E.: Numerical simulation of flow and chemical transport in integrated surface-subsurface hydrologic systems. Ontario, Canada. Ret rieved from: Ph. D thesis. University of Waterloo. http://hdl.handle.net/10012/412, 1999.

VanderKwaak, J. E., & Loague, K.: Hydrologic-response simulations for the R-5 catchment with a comprehensive physics-based model. Water Resources Research, 37(4), 999–1013. https://doi.org/10.1029/2000WR900272, 2001.

AMLR, Water Data Services: Pedler Creek @ Stump Hill Road - A5030543. Retrieved March 10, 2019, from:
610   https://amlr.waterdata.com.au/Flow.aspx?sno=A5030543&Report=, 2019.

Weill, S., Altissimo, M., Cassiani, G., Deiana, R., Marani, M., & Putti, M.: Saturated area dynamics and streamflow generation from coupled surface–subsurface simulations and field observations. Advances in Water Resources, 59, 196–208. https://doi.org/10.1016/j.advwatres. 2013.06.007, 2013.

Wigmosta, M. S., Vail, L. W., and Lettenmaier, D. P.: A distributed hydrology-vegetation model for complex terrain, Water
615   Resour. Res., 30(6), 1665– 1679, doi:10.1029/94WR00436, 1994.

Ye, W., Bates, B. C., Viney, N. R., Sivapalan, M. and Jakeman, A. J.: Performance of conceptual rainfall-runoff models in low-yielding ephemeral catchments, Water Resour. Res., 33(1), 153–166, doi:10.1029/96WR02840, 1997.

620 **Table 1: Hydraulic Mixing-Cell delineated fractions.**

Flow generation mechanism	Fraction name	Fraction origin
Saturation excess overland flow	SE-OF (Dunne)*	River and sand, clay and loam hillslopes
Infiltration excess overland flow	IE-OF (Horton)	In-stream and sand, clay and loam hillslopes
Saturated interflow	Sat-IF	In-stream and sand, clay and loam hillslopes
Unsaturated interflow	Unsat-IF	In-stream and sand, clay and loam hillslopes
Pre-event GW	Pre-event GW (old GW)	Porous media

Note. HMC = Hydraulic Mixing-Cell; IF = interflow; SE-OF = saturation excess overland flow;
IE-OF = infiltration excess overland flow; GW = groundwater.
*Common names used for the fractions are shown in parenthesis

625

Table 2: Surface-Subsurface Parameters for Pedler Creek. See Figure 1 for land use distribution.

Media	Parameter	Value
Surface		
Floodplain Agriculture	Manning's roughness n	4.05 E-7 s/m$^{1/3}$
	Rill storage	0.01 m
	Obstruction storage	0.0 m
Floodplain Pasture	Manning's roughness n	3.47 E-7 s/m$^{1/3}$
	Rill storage	0.01 m
	Obstruction storage	0.0 m
Floodplain Urban	Manning's roughness n	1.85 E-7 s/m$^{1/3}$
	Rill storage	0.01 m
	Obstruction storage	0.0 m
Creek Valley	Manning's roughness n	1.15 E-6 s/m$^{1/3}$
	Rill storage	0.01 m
	Obstruction storage	0.0 m
Creek Headwaters	Manning's roughness n	4.05 E-7 s/m$^{1/3}$
	Rill storage	0.01 m
	Obstruction storage	0.0 m
Surface-Subsurface Coupling	Coupling length	0.001 m
Subsurface		
Sand	Hydraulic conductivity K_{sat}	0.314, 1.06, 7.128 m/d
	Porosity	0.43
	van Genuchten α	5.9, 7.5, 14.5 m^{-1}
	van Genuchten β	1.48, 1.89, 2.68
	Residual saturation θ_r	0.045
Loam	Hydraulic conductivity K_{sat}	0.0624, 0.108, 0.2496 m/d
	Porosity	0.46
	van Genuchten α	1.9, 2.0, 3.6 m^{-1}
	van Genuchten β	1.31, 1.41, 1.56
	Residual saturation θ_r	0.067, 0.095, 0.078
Clay	Hydraulic conductivity K_{sat}	0.0624, 0.0009 m/d
	Porosity	0.475
	van Genuchten α	1.9, 0.6 m^{-1}
	van Genuchten β	1.31.
	Residual saturation θ_r	0.095
Quaternary Sediments	Hydraulic conductivity K_{sat}	0.86301 m/d
	Porosity	0.3
	van Genuchten α	7.5
	van Genuchten β	1.89
	Residual saturation θ_r	0.065
Port Willunga Formation	Hydraulic conductivity K_{sat}	4.1095 m/d
	Porosity	0.3
	van Genuchten α	12.4 m^{-1}
	van Genuchten β	2.28
	Residual saturation θ_r	0.057
Blanch Point Formation	Hydraulic conductivity K_{sat}	8.6E^{-05} m/d
	Porosity	0.3
	van Genuchten α	4.3 m^{-1}
	van Genuchten β	1.25

	Residual saturation θ_r	0.02	
Maslin Sands	Hydraulic conductivity K_{sat}	0.86 m/s	
	Porosity	0.3	
	van Genuchten α	7.5 m^{-1}	630
	van Genuchten β	1.89	
	Residual saturation θ_r	0.065	
Evapotranspiration			
Grass	Evaporation depth	1 m	
	Root depth	1 m	
	Leaf area index	1	
	Transpiration fitting parameter c1	0.5	
	Transpiration fitting parameter c2	0.0	635
	Transpiration fitting parameter c3	1.0	
	Wilting point	0.29	
	Field capacity	0.56	
	Oxic limit	0.75	
	Anoxic limit	0.9	
	Limiting saturation (minimum)	0.25	
	Limiting saturation (maximum)	0.9	640
	Canopy storage parameter	0.0 m	
	Initial interception storage	0.0 m	
Eucalyptus	Evaporation depth	3 m	
	Root depth	5 m	
	Leaf area index (LAI)	2.08	
	Transpiration fitting parameter c1	0.6	
	Transpiration fitting parameter c2	0.0	645
	Transpiration fitting parameter c3	1.0	
	Wilting point θ_{wp}	0.29	
	Field capacity θfc	0.56	
	Oxic limit θ_o	0.8	
	Anoxic limit θ_{an}	0.95	
	Limiting saturation (minimum)	0.25	
	Limiting saturation (maximum)	0.9	
	Canopy storage parameter	0.00045	
	Initial interception storage	0.0003	

Table 3: Properties of tested model scenarios.

Scenarios testing the shallow soils Ksat (m/d)[a]	
Scenario 1	Sand = 1.06
	Loam = 0.108
	Clay = 0.0009
Scenario 2	Sand = 0.314
	Loam = 0.0624
	Clay = 0.0009
Scenario 3	Sand = 1.06
	Loam = 0.0624
	Clay = 0.0009
Scenario 4	Sand =0.314
	Loam = 0.108
	Clay = 0.0009
Scenarios testing the stream incision values (m)[b]	
Scenario 5	4
Scenario 6	6
Scenario 7	8
Scenario 8	10
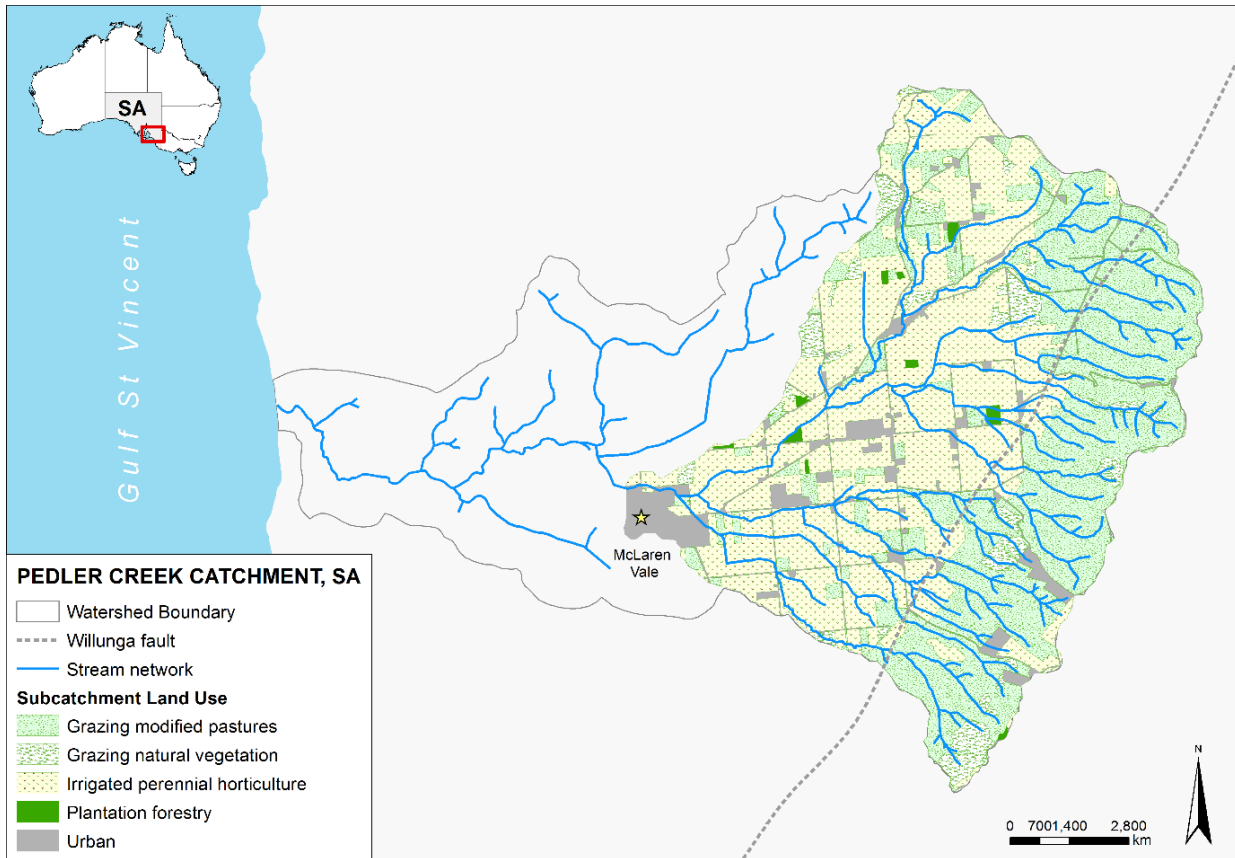
Figure 1: Pedler Creek catchment location showing the original watershed boundary, the stream network, and the Willunga Fault. The five major land uses are shown for the model sub-basin.
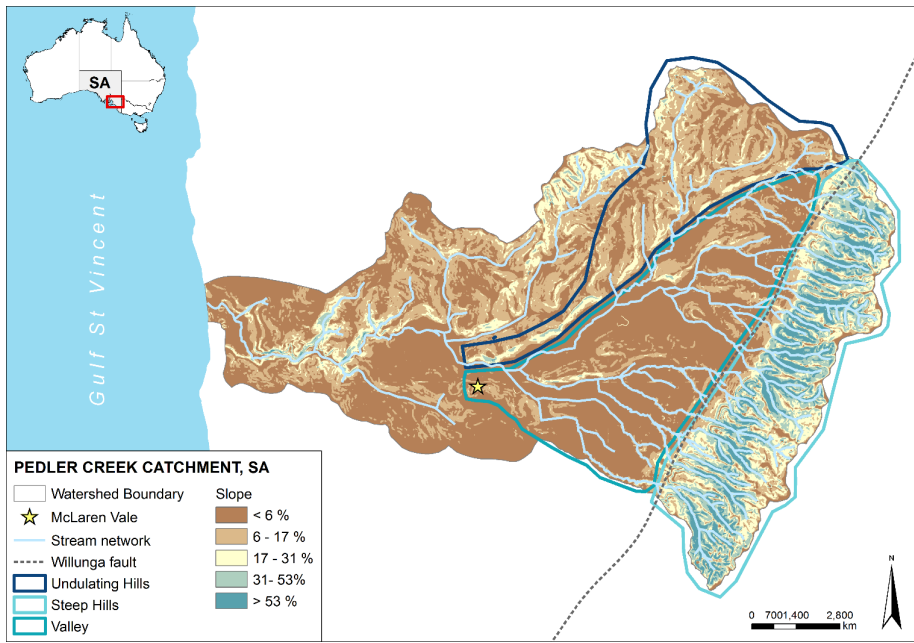
655 **Figure 2: Pedler catchment slopes highlighting the three distinctive areas for the sub-catchment area: undulating hills on the north, the steep hills on the east and the low gradient valley.**
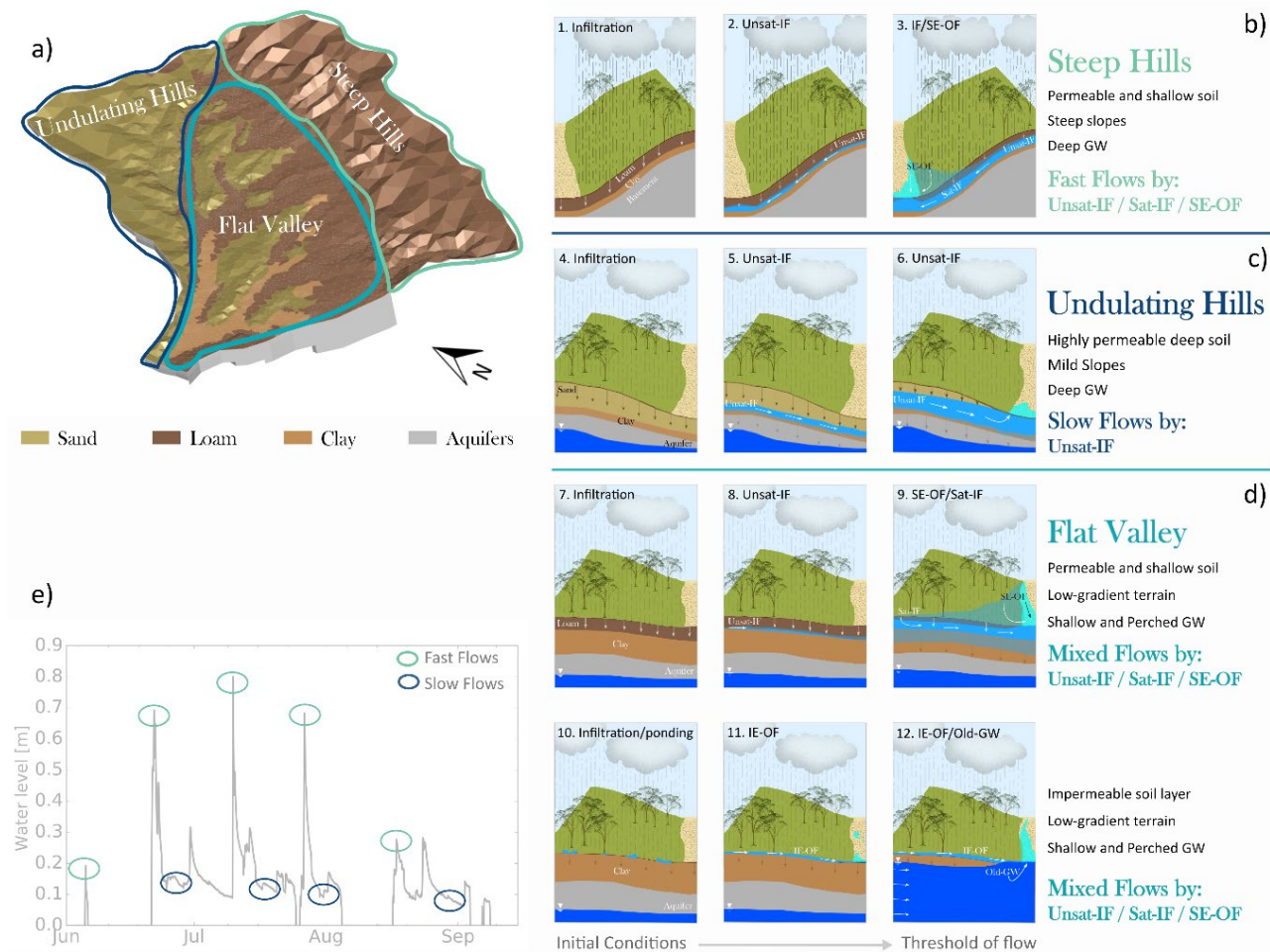
Figure 3: a) Conceptual diagram showing the three major areas that are likely to develop distinct streamflow generation mechanisms during the intermittent flow season. **b-d)** 2D soil profiles for the three major areas detailing the processes developing from the initial conditions until the threshold of flow (modified from Gutierrez-Jurado et al., 2019) e) Typical hydrograph during the intermittent season highlighting the hypothesized 'fast' and 'slow' flow components.

*For illustration purposes, the aquifers are presented as a single unit depicted in grey.

*Arrows represent flow direction
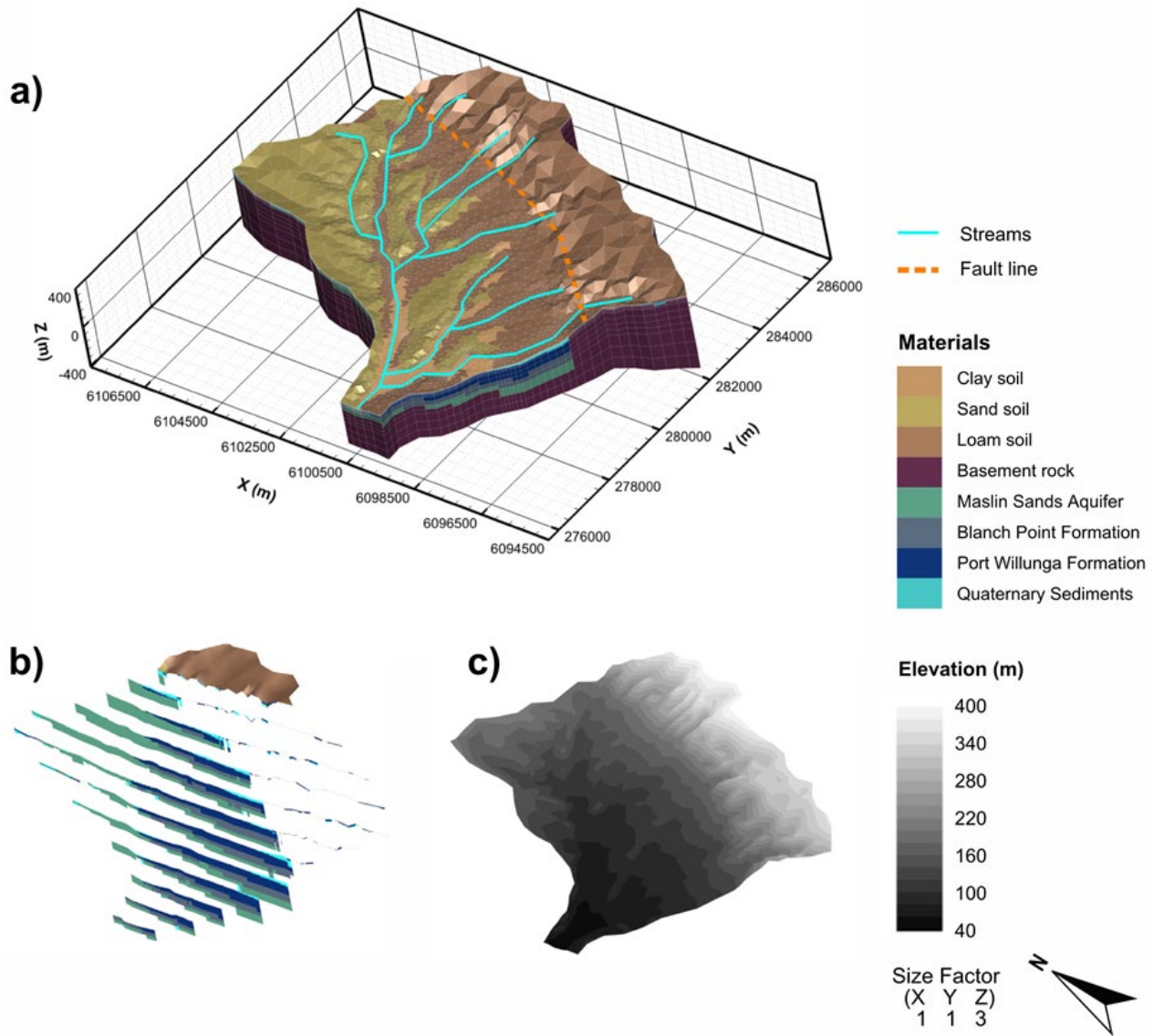
665   **Figure 4: a) Three-dimensional representation of Pedler catchment showing the mesh discretization and the spatial distribution of shallow soil types b) Slices showing the distribution and thickness of the hydrogeological layers. c) Digital elevation model showing the surface topography.**

* Approximated location of the discretised stream network and the fault line are over imposed for illustration purposes.

	[1]	[2]	[3]	[4]	[8]
a)	Area = 27%	Area = 28%	Area = 28%	Area = 27%	Area = 18%

Dominant Fraction

No-Flow | Unsat-IF | IE-OF Loam | IE-OF Clay | Pre-Event GW

In-stream | Hillslope | Porous Media

Saturation

0 0.1 0.2 0.3 0.4 0.5 0.6 0.7 0.8 0.9 1
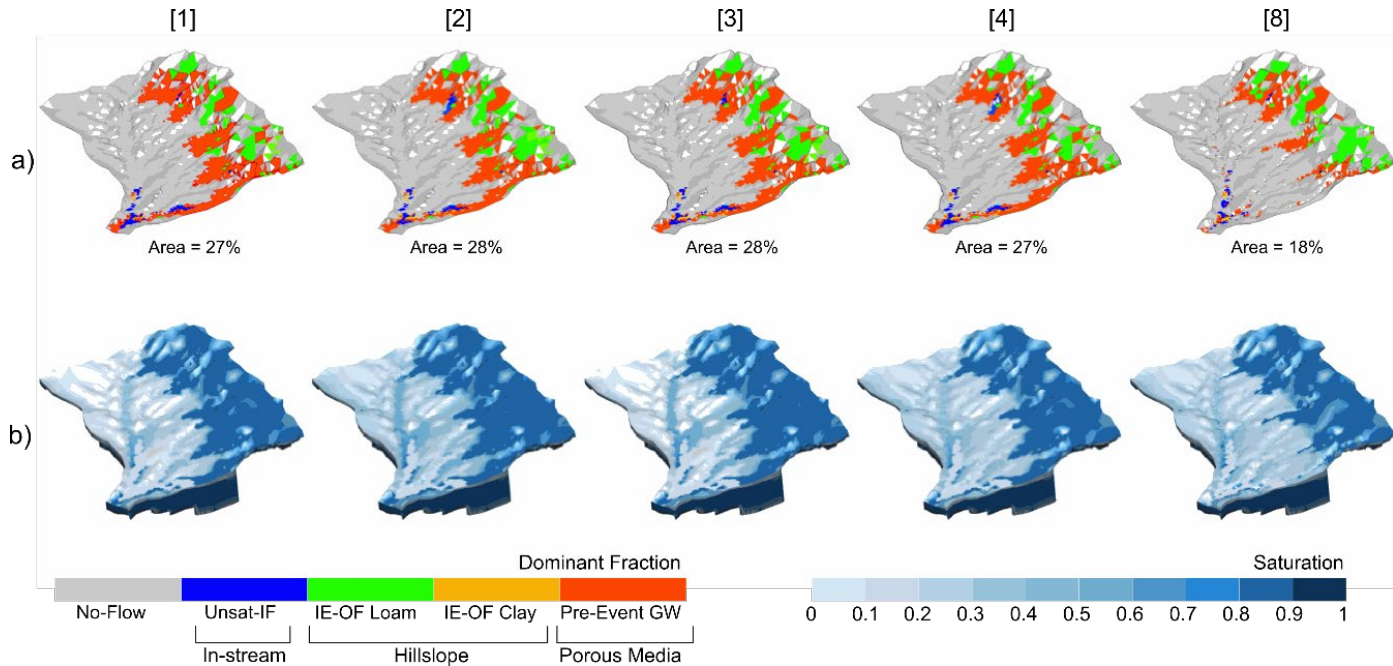
670

Figure 5: Snapshots of time step 960 during a rainfall event showing (a) the spatial extent of active areas by their dominant HMC component (flow generation mechanism) for each scenario (1-4 and 8) and (b) the porous media saturation. The spatial extent of active areas as a percentage of the catchment area is shown below the snapshots. Colours for the HMC components show both the dominant process and the origin of the water contributing to the flow in each cell. For example, all red areas are from Pre-Event GW some of which

675   can contribute to active areas in both the stream and in the stream banks.
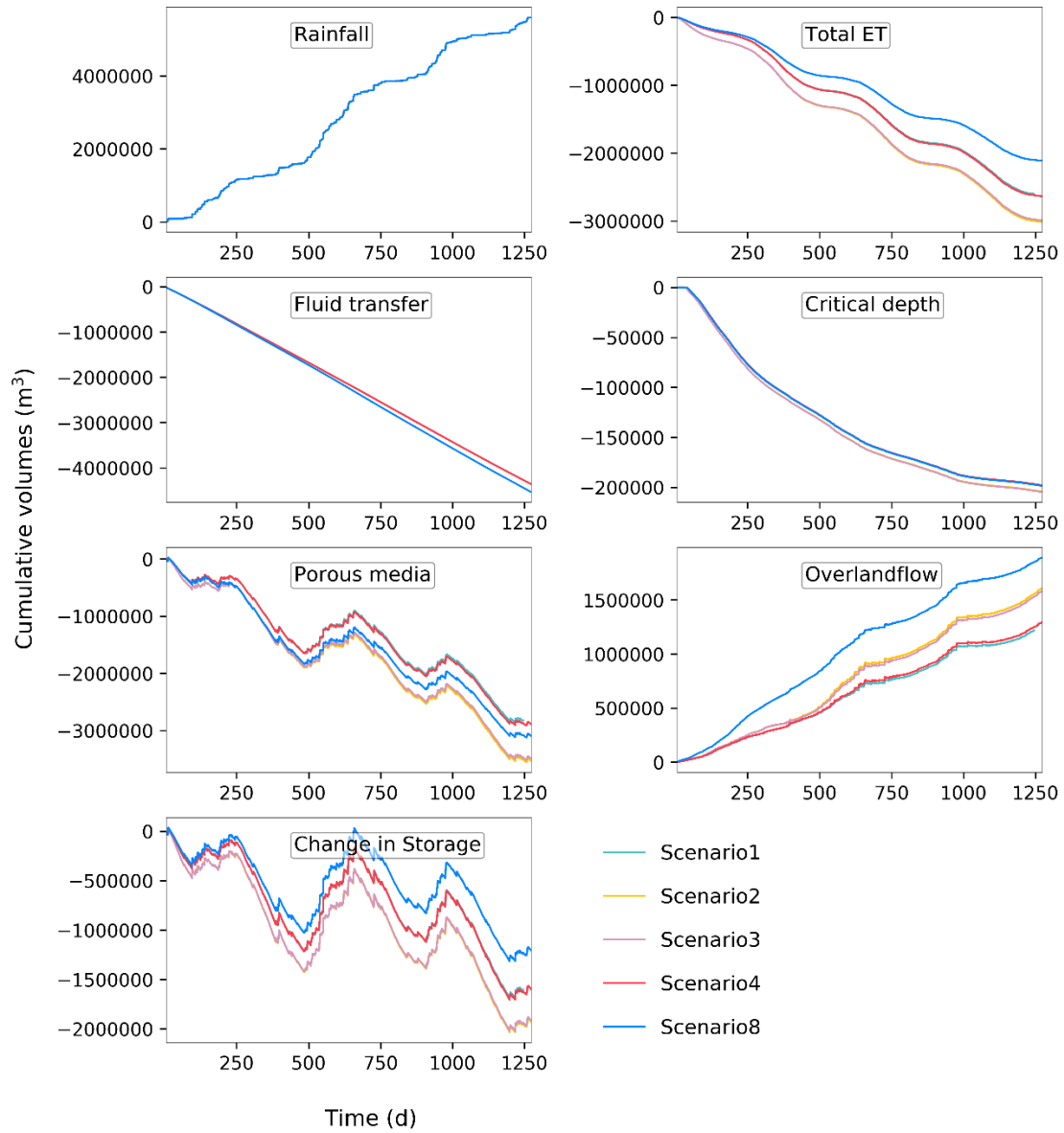
Figure 6: Cumulative values of the water balance components simulated with HydroGeoSphere for scenarios 1-4 and 8.